

Characterization of a Rotational Thrust Balance for Propellantless Propulsion Concepts Utilizing Magnetic Levitation with Superconductors

IEPC-2019-290

Presented at the 36th International Electric Propulsion Conference
University of Vienna • Vienna, Austria
September 15-20, 2019

O. Neunzig¹, M. Kössling², M. Weikert³ and M. Tajmar⁴
Institute of Aerospace Engineering, Technische Universität Dresden, 01307 Dresden, Germany

Abstract: The development, thrust measurement and characterization of advanced electric propulsion systems are crucial to determine their capabilities in future space applications. Especially the increasing scientific interest in large-scale space exploration requires a breakthrough in propulsion physics, since modern systems are insufficient for this task. Within the SpaceDrive-Project at the Institute of Aerospace Engineering at Technische Universität Dresden (TU Dresden), we investigate promising propulsion concepts that do not rely on propellant and therefore eliminate the mission constraints of limited propellant storage within a spacecraft. Among these propellantless propulsion concepts, the EMDrive and Mach-effect thruster (MET) are main subjects of this study. These concepts are not yet confirmed to be functional, thus requiring the need for advanced testing facilities. For this reason, we developed a new kind of rotational thrust balance. The objective is to detect thrusts in the range of $\sim 1\mu\text{N}$ by measuring the change in angular velocity if a magnetically levitated testbed inside a vacuum chamber onto which the thruster applies a torque. Main purpose of the thrust balance is to reduce the propability of false measurements frequently found with torsion balances such as interactions between the thruster and the environment from the earth's magnetic field, vibration through balance components or drifts from center of mass shifts e.g. due to thermal expansion. Therefore, the balance is based on a magnetic levitation bearing utilizing Yttrium-Barium-Copper-Oxide (YBCO) high-temperature superconductors and permanent magnets to provide a frictionless rotational degree of freedom. The main components of the balance, their features and subsequently initial function tests of the EMDrive without the magnetic bearing are presented and discussed.

Nomenclature

a	Angular acceleration [rad/s^2]	J_C	Critical current density [A/m^2]
\vec{a}	Fractional acceleration [m/s^2]	M_T	Torque of the propulsion system [Nm]
B_C	Critical magnetic flux density [T]	R	Thruster lever-arm [m]
$F_{\vec{a},COM}$	Fractional gravitational force [N]	T_C	Critical temperature [K]
F_T	Thrust of the propulsion system [N]	Δt	Time of thruster operation [s]
\vec{g}	Gravitational acceleration [m/s^2]	Δv	Change in velocity [m/s]
i	Rotational plane inclination [rad]	$\Delta\omega$	Change in angular velocity [rad/s]
J	Moment of inertia [kgm^2]		

¹ Ph. D. Candidate, TU Dresden, Institute of Aerospace Engineering, Germany, Oliver.Neunzig@tu-dresden.de

² Ph. D. Candidate, TU Dresden, Institute of Aerospace Engineering, Germany, Matthias.Koessling@tu-dresden.de

³ Ph. D. Candidate, TU Dresden, Institute of Aerospace Engineering, Germany, Marcel.Weikert@tu-dresden.de

⁴ Institute Director, Professor and Head of Space Systems Chair, Martin.Tajmar@tu-dresden.de

Abbreviations

DOF	Degree of freedom
FCD	Field cooling distance
MET	Mach-effect thruster
SC	Superconductor
YBCO	Yttrium-Barium-Copper Oxide

I. Introduction

MODERN space travel is confronted with a ceaseless desire of mankind to explore the universe beyond our solar system. To lay the foundation for interstellar missions within our lifetime, the development of new technologies for the main challenges of this intention are inevitable. Since space travel primarily relies on overcoming enormous distances, there are strong technical requirements for propulsion technologies. Despite continuous advancements in space propulsion systems, present systems no longer meet the desired performances for large-scale missions. Sir Isaac Newton's third law of motion and the Tsiolkowsky's rocket-equation confine their realm of feasibility towards large Δv with on-board propellant. There is a strong need for a breakthrough in propulsion physics.

A novel approach for this challenge are propellantless propulsion concepts. Systems like solar sails and beamed laser propulsion¹, that utilize radiation pressure of the sun or lasers from earth, do not rely on stored propellant. However, they are constricted due to their extrinsic source of energy. The EMDrive^{2,3} and Mach-effect thruster^{4,5} are believed to excel these systems in terms of thrust neither by relying on external energy sources nor on-board propellant to propel a spacecraft. Unlike solar sails, these concepts are not yet confirmed to be functional, but they could lead to a breakthrough in propulsion physics.

Direct measurement of the proposed tiny forces in the vicinity of sub-micronewton is a crucial objective when it comes to investigating and characterizing these concepts in a laboratory environment. Reliable measurement principles have to withstand any kind of doubts one could have either with the principle itself, the setup or most importantly measurement errors due to environmental influences in the mechanical measurement process. Such influences must be detected eliminated from measurement if possible. The single most popular measurement principle for electric propulsion systems are torsional balances. At the Institute of Aerospace Engineering at TU Dresden thorough investigations of these concepts lead to the development of advanced testing facilities. With a precise torsional balance thrusts in the range of μN have been observed for the EMDrive, that could be subject to false measurements due to interactions with earths' magnetic field^{6,7}.

To verify measurement artefacts and reduce the probability of false measurements, a new kind of rotational thrust balance was developed and is presented in this paper (Fig. 1). It is designed to provide a space-like frictionless testbed to investigate propulsion concepts by enabling the possibility to accelerate along a circular trajectory within a vacuum chamber. The ability to perform full rotations leads to advantageous properties with respect to stationary thrust balances by visualizing the performance of mechanical work of the propulsion system, thus removing possible doubts of the functionality of the concept.

Thrust forces are calculated by measuring the change in angular acceleration of the frictionless circular motion. The difficulty in providing motion of large masses with forces in the range of $\sim\mu\text{N}$ is friction within the bearing.

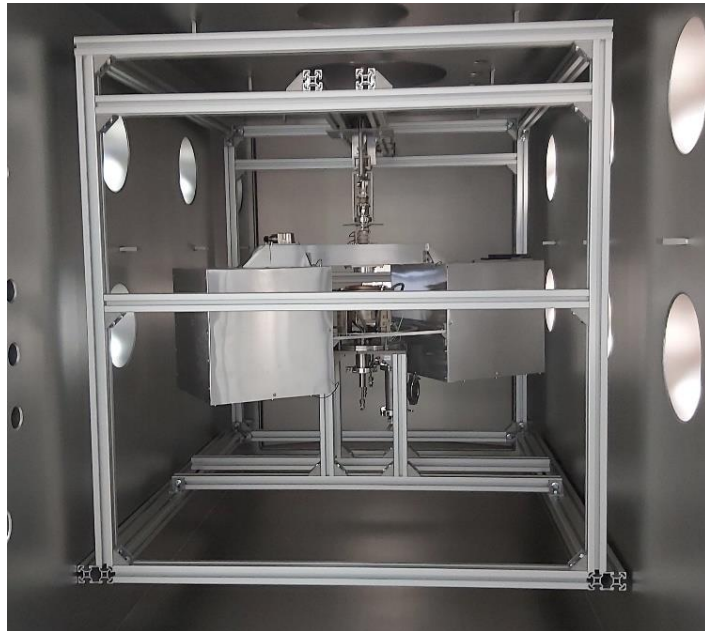


Figure 1. Rotational thrust balance. Position of the rotational thrust balance within its aluminum frame inside the rectangular vacuum chamber at TU Dresden.

Components like ball bearings are orders of magnitude above the tolerable frictional forces and therefore unsuitable. To overcome this issue, the balance is based on magnetic levitation.

A notable example of a magnetically levitated thrust balance is the system developed by F. Mier-Hicks and P. C. Lorenzo⁸ at MIT. Their approach is an electromagnetically levitated balance for CubeSats with Electro Spray thrusters, which is capable of $\sim\mu\text{N}$ thrust measurements for a levitated mass of up to 1 kg.

The rotational thrust balance presented in this paper was developed for thrust measurements in the range of micronewtons while it is able to levitate a mass of up to 22 kg. In order to reach these properties the balance utilizes the unique properties of superconductivity. We developed a magnetically levitated testbed for propulsion systems of interest by utilizing the superconducting material combination of Yttrium-Barium-Copper-Oxide (YBCO), which loses its electrical resistivity at 92 K in combination with a cylindrical permanent magnet. A brief description of the SC-phenomenology and their implementation in the setup is presented in chapter II. To access the superconducting properties of YBCO over a long period, the facility features a cryostat with a liquid-nitrogen heat exchanger, presented in chapter III, A.

Determined by the combined properties of cylindrical permanent magnets and superconductors to retain one remaining degree of freedom, the rotational plane of the balance must be levelled below a threshold of 0.01° to enable full rotations of a levitated mass of 22 kg with only $1\mu\text{N}$ of thrust. A detailed description of the levelling procedure prior to measurements is presented in Chapter III, C.

To investigate the properties of the rotational thrust balance in combination with a propulsion system, initial functionality tests with the EMDrive are presented and discussed. These tests had the intention of detecting disturbances in the test-setup, especially among the complex alignment mechanisms of the balance. The results presented have yet to be confirmed with additional measurements.

II. Superconductivity and measurement principle

The thrust measurement principle in general is based upon analyzing the change in angular velocity of a rotating mass. Therefore, the most important and challenging task to create a real test stand is the requirement to develop a bearing that provides close to zero friction. Allowing a mass to accelerate along a circular trajectory with micronewtons of thrust strongly depends on the properties of the bearing in the rotational axis of the system. The frictional torque of components like ball bearings is magnitudes above the tolerable friction for the balance. To meet these requirements we approached the zero friction requirement by utilizing magnetic levitation. Magnetically levitated components offer the lowest frictional torque due to the non-existing mechanical contact of the components. As mentioned before, magnetic levitation with conventional electromagnets was insufficient for all the requirements of the test stand, especially the long-time levitation of masses up to 20 kg. The system of choice is a combination of a cylindrical NeFeB permanent magnet and the unique properties of superconductivity with YBCO high-temperature superconductor discs. This system is commonly used for high-speed rotational applications like energy storage in flywheels with minimal energy losses due to the frictional torque that is almost nonexistent.

Ideal superconductors below their so-called critical temperature T_c have the ability to conduct electrical currents without resistivity whatsoever. This property leads to unique electromagnetic interactions with external magnetic fields. If a superconductor is cooled below its critical temperature in presence of an external magnetic field from a permanent magnet, it acts like a magnetic mirror. The material combination of YBCO belongs to the type-II high-temperature superconductors. The properties of

this type divides into three main characteristics during the cooling process (Fig. 2). While the superconductor is above its critical temperature (Fig 2, a), there are no interactions with external magnetic fields and the SC. In phase two of the cooling process, the SC reaches its critical temperature, hence enabling the superconducting properties. As long

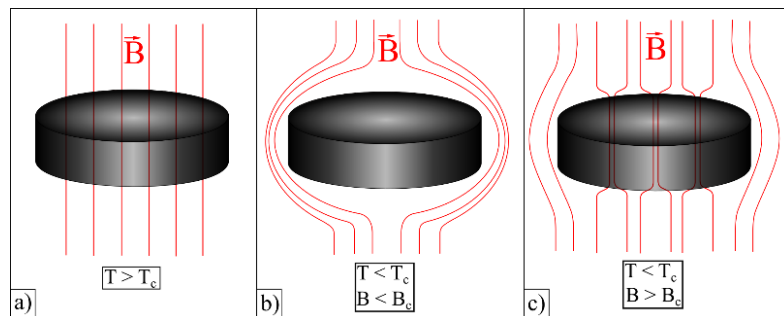


Figure 2. Properties of Type-II superconductors. a) Above the critical temperature (normal phase); b) below the critical temperature (Meissner-state); c) above the critical magnetic flux density (vortex phase).

as the maximum current density j_c inside the SC does not exceed the threshold, it stays in the so-called Meissner-state and repels external magnetic fields from its core (Fig. 2, b). If the external magnetic field exceeds a critical flux density B_C , the current density of the SC surpasses its critical limit and reacts with the formation of so-called flux tubes (Fig 2, c). At these positions, the magnetic field penetrates the SC locally and locks the magnetic field in position through the generation of flux vortices in the vortex-phase⁹. In this state, cylindrical permanent magnets are magnetically restricted in their motion by solely leaving a rotational degree of freedom (DOF) and creating spring-like stiffness in radial and axial directions that increase with lower temperatures (Fig 3). The superconductor is submerged within a bath of liquid nitrogen to reduce its temperature to -196°C while the permanent magnet passively levitates above. In comparison to electromagnetically levitated magnets, this system offers an increased axial load capacity on a smaller construction volume, while not depending on closed-loop control of the electromagnetic coil. Downside of the superconducting levitation is an increased constructional complexity for a cryostat in order to keep the superconductor below its critical temperature while it is in a vacuum environment. A detailed description of the cryostat is presented in chapter III, A.

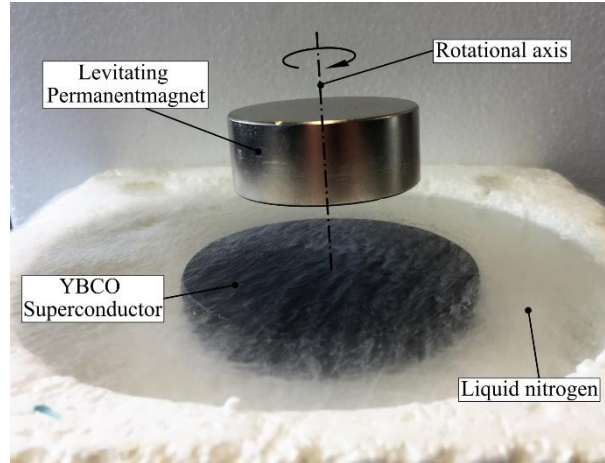


Figure 3. Passive magnetic levitation. *Levitating permanent magnet above an YBCO superconductor submerged within a reservoir of liquid nitrogen.*

The rotational DOF remains due to the rotationally symmetric magnetic field lines of the cylindrical magnet. The axial load capacity strongly depends on the distance between the SC and the magnet while reaching the critical temperature. This distance is defined as the field cooling distance (FCD).

The superconductor on its own does not withstand multiple load cycles due to its ceramic structure. Therefore, we strengthened the material with a thin layer of STYCAST, a two-component adhesive that reinforces the mechanical structure and prevents it from outgassing and degrading its properties in a vacuum environment.

This system is the basis of the rotational thrust balance. The propulsion systems of interest are placed onto the levitating magnet with a dedicated lever-arm. The propulsion system applies a force onto the levitating lever-arm, which leads to a torque onto the levitated magnet (Fig 4). Any gain in angular velocity must be detected to calculate the applied force. In an ideal frictionless environment, basic physics is needed to calculate the produced thrust by knowing the moment of inertia of the levitated structure J , the gain in angular velocity $\Delta\omega$, thruster lever-arm R , and the amount of time Δt of thruster operations. The thrust is then calculated by using equation (1)-(3).

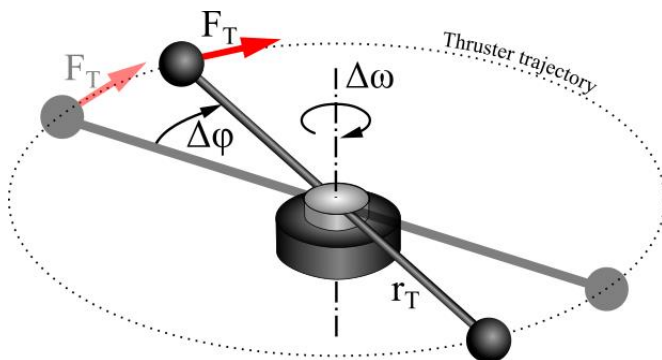


Figure 4. Thrust measurement principle. *Schematic of the rotational thrust measurement principle by analyzing the change in angular acceleration of a propulsion system along a circular trajectory.*

$$M_T = F_T \cdot R = J \cdot a \quad (1)$$

$$a = \frac{\Delta\omega}{\Delta t} \quad (2)$$

$$F_T = \frac{J \cdot \Delta\omega}{R \cdot \Delta t} \quad (3)$$

It is important to notice, that the non-ideal rotational behavior includes disturbing factors, that have to be taken into account during measurements regarding frictional torque. The performance of the magnetic bearing is constrained by the quality of the permanent magnet and the trapped magnetic field inside the superconductor. Either of which could possess inhomogeneities in their flux density distribution across their surface. These

inhomogeneities could lead to magnetic forces that interfere thrust measurements. For this reason, the magnetic flux densities of the bearing parts were measured experimentally and their influence in measurements will be investigated through measurements.

Due to the fact, that the superconducting levitation leaves only one degree of freedom, there is a significant dependency between the ability to perform full rotations and the inclination of the corresponding rotational plane of the system. Insufficient alignments of the center of mass of the levitating structure lead to complications in thrust measurements by introducing a scaling factor of the gravitational acceleration within the rotational plane.

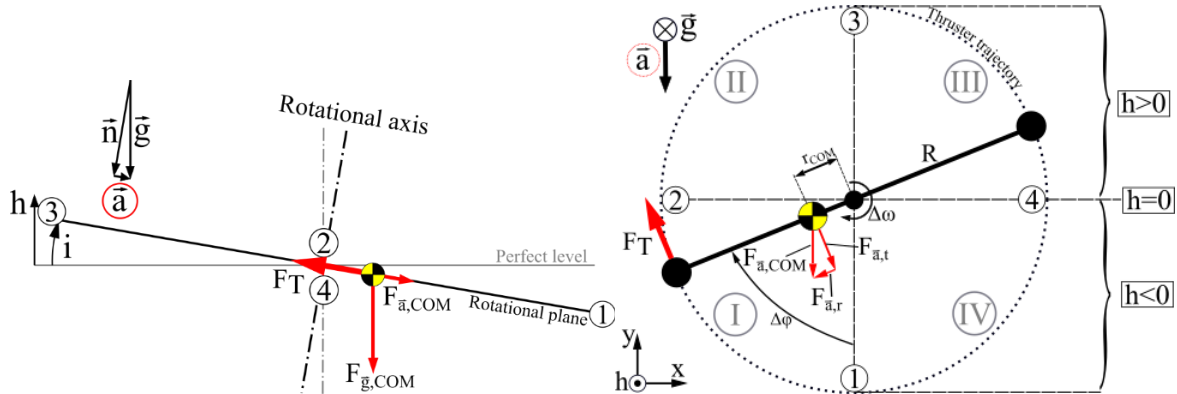


Figure 5. Inclination of the rotational plane. *Left:* Lateral view of the rotational plane with a misalignment of the center of mass outside the rotational axis. *Right:* Top view of the rotational plane with a restoring torque due to the center of mass misalignment against the thrust direction.

This fraction interferes with measurements by preventing full rotations due to a restoring gravitational force that scales with the levitated mass and the inclination. Critical misalignments of levitated masses may prevent any rotation whatsoever. In this case the thruster would deflect the levitating system to a certain position and reaches a point of force equilibrium between thrust and gravitational force. The absence of the magnetic bearings self-leveling ability restricts the value for the remaining fraction of the gravitational acceleration according to equation (4).

$$\vec{a} = \vec{g} \cdot \sin(i) \quad (4)$$

The relation is illustrated in figure 5 (left) with a lateral view of the rotational plane. Positions 1-4 indicate different positions of the center of mass that are used to describe its influence on thrust measurements within this chapter. Thrust measurement take place either by averaging the thrust for the total sum of performed rotations in time, by analyzing one isolated rotation or by observing small angular changes in position. In the case of thrusts close to the resolution of the balance, it is beneficial to derive the continuous thrust by small deflections rather than full rotations. Therefore, the rotational plane is dissected into four different quadrants, either of which with a different influence of the rotational plane inclination (Fig. 5, right). In quadrants I-II the fraction of the gravitational force $F_{\vec{a},COM}$ opposes the thrust F_T provided by the propulsion system, hence slowing the circular motion. In quadrants III-IV the gravitational force supports the angular velocity. Position 1 indicates the resting position of the center of Mass, where the rotational plane is at its lowermost position within the gravitational field ($h = \text{minimum}$). This position is a stable equilibrium between gravitational force of the center of mass due to the fractional amount of gravitational acceleration A and the inclination of the rotational plane. Positions 2 and 4 exhibit the largest influence in thrust measurements due to a maximum in restoring torque, that counteracts the thrust vector of the propulsion system. Especially location 2 determines the minimum thrust for a full rotation, because gravitational torque is at its maximum. Similar to position 1, the location indicated with 3 is an equilibrium at the highest position within the gravitational field, therefore it is unstable. These constraints of measurement in the lower thrust range fortify the importance of rotational plane leveling. For that purpose, we integrated a mechanical system to level the rotational plane of the thrust balance that is described in chapter III, C.

III. Thrust stand components

The thrust balance was developed to magnetically levitate a propulsion concept of interest and the supporting frame with a total mass of up to 22 kg inside a vacuum chamber. In order to provide full rotations for the thruster with expected thrust forces in the range of μN , the rotating plane of the circulator trajectory must not exceed a deviation from the perfect level of 0.01° as described previously. For this reason, the facility features a leveling-mechanism with a double pivot-bearing, allowing oscillations in two axis due to the cardanic suspension. A detailed description of the combined leveling and lifting mechanisms is presented in the subsection C of this chapter. With moveable masses inside the electronics box, the centre of mass of the levitating frame can be adjusted to fit the requirements for a full rotation. An inclination sensor on the main supporting beam provides telemetric data to observe the levelling process.

The main parts of the magnetic bearing are a cylindrical permanent magnet and a superconductor inside a cryostat with a reservoir of liquid nitrogen. The bearing enables almost zero-friction along a single rotational degree of freedom (subsection A). With liquid metal contacts, the electronics and thruster can be supplied with electrical power while performing full rotations (subsection D). A high precision optical sensor tracks changes in angular position in order to derive its angular position to derive the actual thrust force along its trajectory (subsection E). The following subsections will provide a detailed look at most crucial parts for the functionality of the balance (Fig. 6). The basic motion of the rotating system is illustrated in figure 6 A-C.

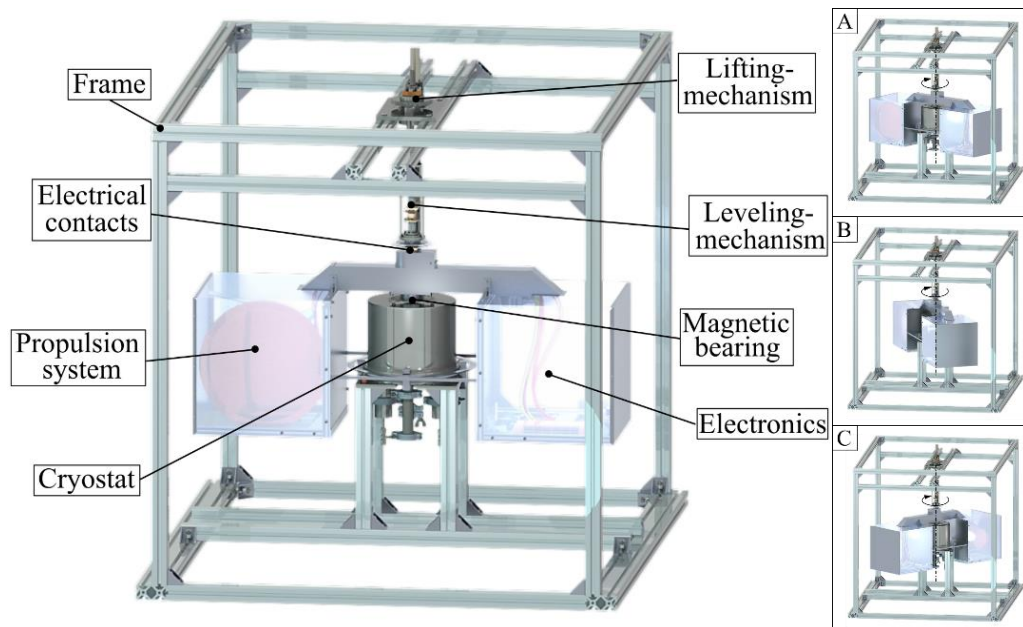


Figure 6. Main components of the rotational thrust balance. *Left:* Indication of the main components. *Right (A)-(C):* Illustration of the circular motion within the aluminum frame.

A. Cryostat

Two different sizes of YBCO high-temperature superconductors are available for the balance. Both of which with a height of 16 mm and outer diameters of 54 mm/80 mm. YBCO has a critical temperature of 92 K that needs to be reached in order to access the superconducting properties. This type of bearing is able to provide an axial load capacity of up to 22 kg while maintaining one rotational degree of freedom with almost zero-friction. To access the superconducting properties of Yttrium-barium-copper-oxide over a long period, the material requires a continuous cooling below its characteristic critical temperature of 92 K. For this reason, the testbed features a liquid nitrogen cryostat. In general, this device contains a heat exchanger of various shapes and thermal insulation techniques to reduce the required amount of energy. There are three distinct function principles commonly used for cryostats, like the flow-cycle and bath cryostat that utilize liquid nitrogen as a cooling medium. On the other hand, there are systems like cryocoolers that obtain cryogenic temperatures with a refrigerating process. The thrust balance presented in this paper features a heat exchanger with a liquid nitrogen bath-cryostat (Fig. 7, right).

Two fabric tubes supply the reservoir with liquid nitrogen through ascension tubes. The reservoir itself is a welded stainless steel containment with a copper cold head, which is hard-soldered into the cover-plate. A third tube, welded to the bottom of the reservoir, serves as a drain valve to quickly clear the reservoir of remaining nitrogen in cases of failure or early measurement terminations. Otherwise, the insulation would prevent the nitrogen to vaporize in a manageable time. Two superconductors of different sizes are positioned within the cold head and fixated with a copper socket. Eleven copper plates are hard-soldered to the underpart of the cold head and immersed into the liquid nitrogen. This arrangement exchanges the heat from the superconductor with the liquid nitrogen to cool it below its critical temperature.

At 1 Bar of atmospheric pressure liquid nitrogen evaporates due to the absorbed heat of the surrounding materials. To prevent the containment from exceeding its pressure limits the evaporated nitrogen exits through one of the supply tubes. Exposed to 1 Bar of atmospheric pressure, liquid nitrogen boils at a temperature of 77 K. By lowering the atmospheric pressure inside the nitrogen reservoir with a vacuum pump, the boiling temperature reaches a minimum of 63 K while it undergoes a phase-change from liquid to solid. With this enhancement, the temperature of the superconductor further decreases, which leads to an improved levitating force and radial stiffness of the bearing.

The reservoir is covered in multi-layer-insulation to minimize heat losses through radiation. A stainless steel housing around the superconductor and liquid nitrogen reservoir can be depressurized in order to reduce heat losses due to convection. This enhancement provides the ability for tests outside of the vacuum chamber by protecting the components from air exposition and the formation of ice on cold surfaces due to humidity.

To handle the axial load of the levitating structure of up to 22 kg, the reservoir is reinforced with four supporting pillars that are fixated to the external frame. A large section of these pillars is made of PEEK. This material features a large tensile strength at cryogenic temperature while reducing heat losses through thermal conduction. With thermocouples (Type-K) the temperature can be measured at five positions to observe the heat distribution (Fig. 7, left).

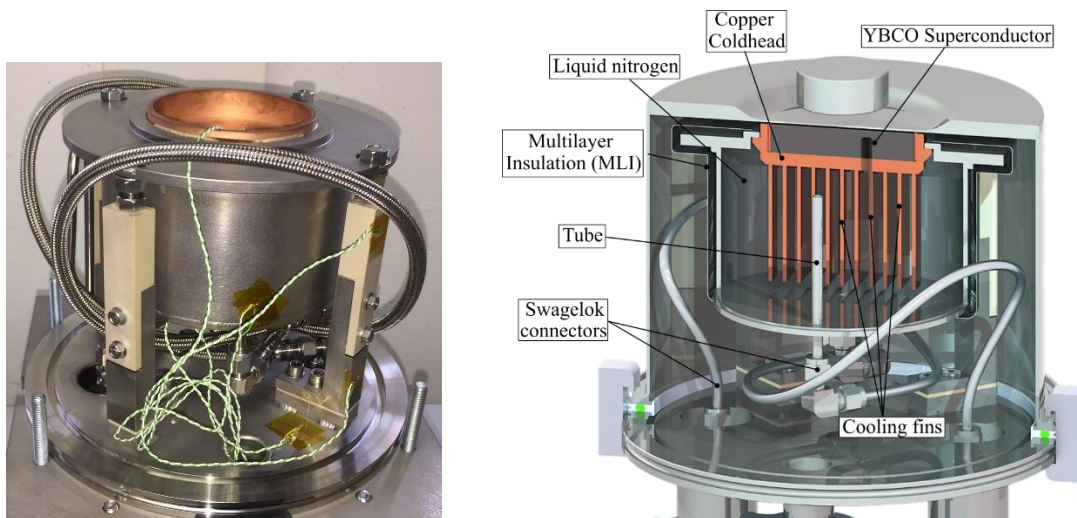


Figure 7. Cryostat. *Left: Exposed reservoir for liquid nitrogen without multilayer insulation and housing. Right : Illustration of the heat exchange mechanism with a sectional view of the liquid nitrogen reservoir with two ascension pipes and copper cooling-fins to cool the superconductor.*

Although the frictional torque of the rotational DOF is the most important characteristic of the magnetic bearing, there is another factor involved in its capabilities. The axial magnetic force of the superconductor constrains the maximum combined weight of the propulsion system and the structural mass. Therefore, axial magnetic force measurements have been conducted with both YBCO superconductors in combination with the cylindrical permanent magnet.

For this process, the superconductor was cooled below its critical temperature without external magnetic fields in close proximity. This so-called zero-field-cooling procedure enables the superconducting Meissner-state, hence repelling external magnetic fields from its core. With a testing-facility, the permanent magnet was forced to a distance down to 1 mm towards the SC and returning to the initial position while analyzing the needed force for each distance. There is a squared dependency of the magnetic force and the distance between the components, reaching a maximum

axial force of 250 N at a distance of 1 mm. The same procedure was conducted with a field-cooling height of 30 mm, leading to a slight decrease in the maximum axial force of 220 N, thus constraining the limits of the levitating structure to 22 kg.

B. Support structure and thruster containments

The total load capacity of the magnetic levitation bearing had to be taken into account for selecting materials for the structural parts of the balance. To design the structure as lightweight as possible, thus providing a large margin for the thruster weight, the supporting frame and containments for thruster and electronics are made of lightweight aluminum profiles. The middle aluminum beam contains the cable management from the liquid metal contacts to the electronics and thruster containment (Fig. 8, right). To create a sufficient resistance against the bending moment of the thruster weight, the beam features a wall thickness of 3 mm and a rectangular profile. While reinforcing the structure, the aluminum containments around the electronics and the thruster act as a faraday-cage to shield any electrostatic interactions between the electronics and the environment inside the vacuum chamber (Fig. 3;4). Otherwise, these interactions may lead to measurement errors. The magnetic field of the permanent magnet is very sensible towards magnetic materials in close vicinities. Distortions of the magnetic field lines could lead to complications during measurements. For that reason, every part of the thrust balance is made of either stainless steel and aluminum or other non-magnetic materials like PEEK and copper.

While not cooled below a temperature of 92 K, the superconductor does not interact with the permanent magnet whatsoever, thus disabling the magnetic levitation. During these phases, the rotating part of the balance supported by a mechanism that is fixated to a frame and surrounds the whole balance. This frame is made of rigid 40x40 mm aluminum beams and represents the balance basis inside the vacuum chamber.

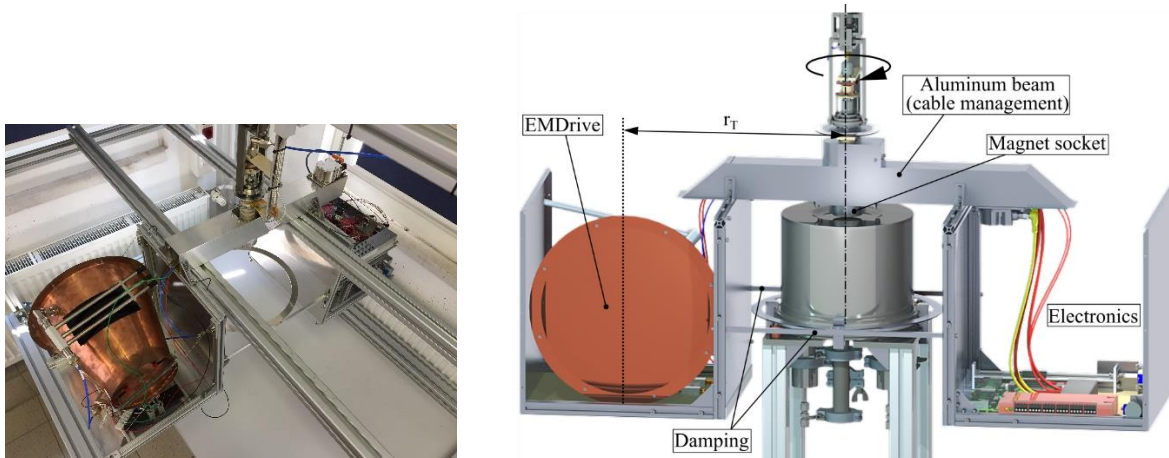


Figure 8. Main structural components of the Thrust balance. *Left: Exposed EMDrive mounted to the containment box and supported by counterweights on the electronics side. Right: CAD image of the main aluminum beam that supports the thruster containment and the electronics.*

Whilst maintaining the zero friction environment of the levitating structure inside the vacuum chamber, any amount of acquired angular momentum leads to a rotation of the system. To counteract this motion during alignments or decelerations of the levitated structure, a controllable damping system is installed to the balance. Four electromagnets with iron cores are fixated to the non-rotating part of the balance. A circular sheet of Aluminum is fixated to the rotating structure and moves in close distance to the electromagnet (Fig. 8, right). Any form of magnetic field originating from the electromagnets, penetrates the aluminum ring. If the electromagnet and the aluminum ring are at rest with respect to each other, this system has no influence on the movement whatsoever. Any motion of the plate induces electrical currents within the aluminum plate perpendicular to the magnetic field lines of the electromagnet due to Faraday's law of induction. These eddy-currents lead to damping forces, counteracting unwanted movements of the levitated structure.

C. Leveling mechanism

As described in chapter II, precise alignments of the permanent magnet and the superconductor in terms of field cooling distance and coaxial orientation must be conducted prior to the measurements. Due to operations inside a vacuum chamber, this alignment-process requires remote-controlled positioning systems. For this reason, the facility features an adjustable mechanism that consists of a leading screw on a spindle to adjust the FCD with a stepper-motor and tune the desired parameters (Fig. 9).

A system with one degree of freedom constrains its self-leveling ability and depends on active adjustments. Therefore, the levitating structure is levelled with inclination sensors and moveable masses. For this reason, the spindle is mounted onto a double pivot bearing to make sure, that the structure is able to align its center of mass within the rotational axis. Two moveable masses inside the electronics box can be adjusted with stepper motors to manipulate the center of mass of the levitating structure. Thereby, the rotational plane can be levelled to the desired value. A *IFM-JN2201* inclination sensor with a resolution of 0.01° observes the inclination of the rotational plane while adjusting the center of mass.

After the levelling process inside the vacuum chamber, the next step is to enable the magnetic levitation by cooling the superconductor with liquid nitrogen below its critical temperature. Subsequently, the spindle mechanism is lowered until the gravitational force of the levitating system is completely transferred to the magnetic levitation force. At this point, the holding mechanism loses contact with the rotating components and the balance is prepared for operations.

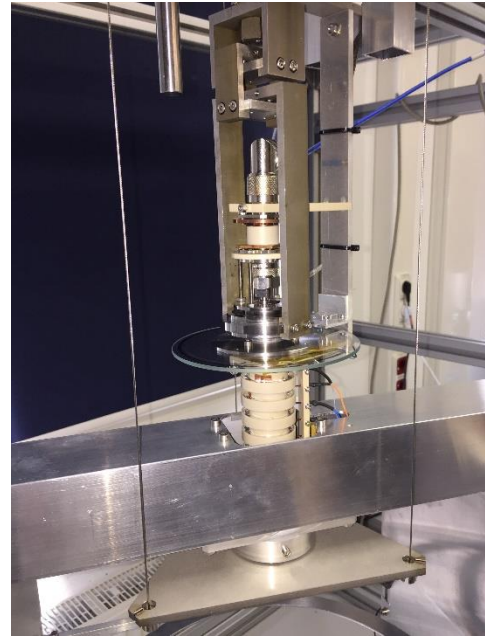


Figure 9. Leveling- and lifting mechanism. *The leveling above the electrical contacts with a double pivot cardanic suspension for free oscillations in either direction.*

D. Electrical power supply

In order to operate the thrusters and electronics, electrical energy is delivered to the balance through liquid metal contacts. Measuring small movements of the balance as a result of thrust is very sensible towards any kind of stiff connections and wires to the frame. Every wire from the power supplies to the propulsion system disturbs measurements by preventing deflections due to stiffness of the wire materials. To counteract this problem, the balance features a power feedthrough utilizing a metal alloy called Galinstan, which is liquid at room temperature and exhibits a very low vapour pressure to operate in a vacuum environment. The rotationally symmetric containments made from Polyether ether ketone (PEEK) are positioned above each other as close as possible to the rotational axis of the system and fixated externally. Copper-pins from the rotating frame are submerged inside the Galinstan to provide on-board power as well as data acquisition (Fig. 10, left). Additionally, a coaxial high frequency contact is positioned within the rotational axis of the system, that is needed to operate the EMDrive and MET.

The constraint of continuous power supply to the balance while performing rotations leads to an influence in measurements. The liquid metal contacts supply electrical energy during rotations while being submerged within the liquid metal. This is the only direct contact between the rotating system and the external frame, besides the magnetic repulsion from the superconductor. As a consequence of the moving pins inside the liquid metal during rotations, liquid friction is induced to the measurements. This friction strongly depends on the lever arm of the copper pins and the angular velocity, upon which the fluid friction scales. This frictional component was quantified in the development process of the balance and is considered in the thrust measurements, although simulations offered negligible results. A more detailed CAD illustration of the liquid metal contacts is presented in figure 10 (right).

With initial functionality tests of the balance in combination with the EMDrive, the communication and continuous power-supply was intact over the whole duration of the test.

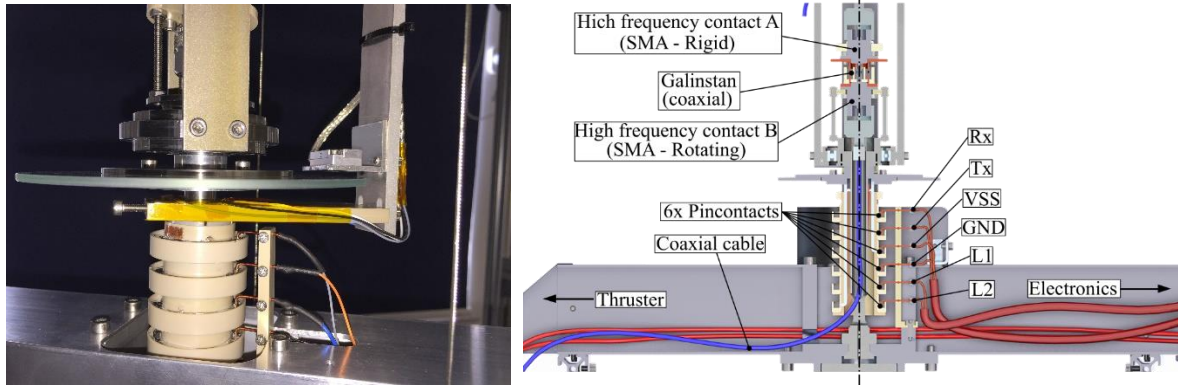


Figure 10. Electrical power feedthroughs. *Left: Rotationally symmetric containments for liquid metal (Galinstan) to serve as contacts for copper-pins on the rotating system that are submerged inside the liquid... Right: CAD image of the coaxial high frequency contact within the rotational and six single pin connectors submerged in Galinstan to feed the thruster and electronics.*

E. Angular sensor

In order to derive the actual force of the thruster along its trajectory, the balance features a high precision optical sensor to track its angular position without direct contact. System of choice is the *Mercury II-6000-V* angular sensor by *MicroE Systems* that consists of a glass-scale with a diameter of 120 mm and 16384 physical counts per revolution at its lowest resolution and an optical encoder (Fig. 11). The encoder tracks corresponding counts to derive a relative position change that is needed for the calculations. With individual interpolation factors, the resolution of the sensor can be set to the desired value with 2.1 arc seconds at best. To calibrate the encoder for complete rotations, the levitating systems rests on a ball-bearing within the leveling mechanism. With this feature, one can manually turn the whole system and and verify the tolerable distances between the sensor and the glass-scale. While the superconducting bearing is inactive, the system is suspended by the double pivot bearing, thus, enabling the rotational sensor to act as a tilt indicator, that can be used to verify the tilt direction measurements of the *JN2201* tilt sensor. Due to the cardanic suspension, center of mass shifts of thrust is able to deflect the suspension which leads to a relative motion between the externally fixated encoder and the glass-scale, that is fixated to the oscillating system. This principle was used to verify the functionality of the sensors during first measurements by operating the EMDrive on the balance with an inactive superconductor. The results of these pretests are presented in the next chapter.

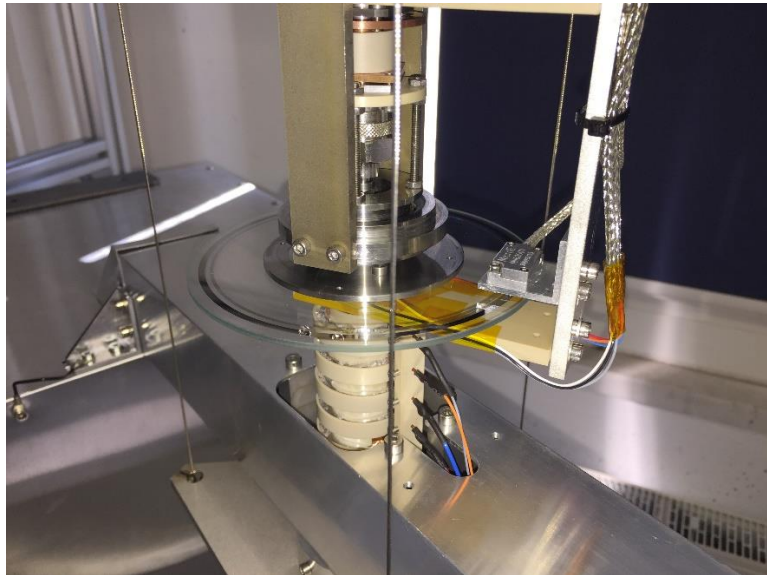


Figure 11. Angular sensor. *The externally fixated Mercury II-6000-V angular sensor by MicroE Systems and a glass-scale with 16384 counts per revolution that is fixated to the rotating system.*

IV. Measurement process and function tests with the EMDrive

At the time of this publication, thrust measurements with the superconductor did not yet take place. Instead, the measurements presented in this chapter are first function tests to investigate interactions between a propulsion concept like the EMDrive and the rotational thrust balance to examine their interaction during operation. Because of the ongoing thermal tests of the cryostat, the superconductor did not yet levitate the system, but its properties were characterized with respect to axial load capacity and magnetic flux density distribution as described in previous chapters.

Instead of levitating the system for measurements, the system was in its levelling-mode by hanging on the cardanic suspension while resting on the ball bearing that is used to calibrate the angular sensor. In this state, a measured deflection originates either from a thrust that is capable of overcoming the frictional torque of the ball bearing or a force that deflects the cardanic suspension in a distinct direction without rotation. In addition, expansion of thermally stressed components of the balance could lead to shifts of the center of mass that deflect the suspension as well, resulting in a measurement signal.

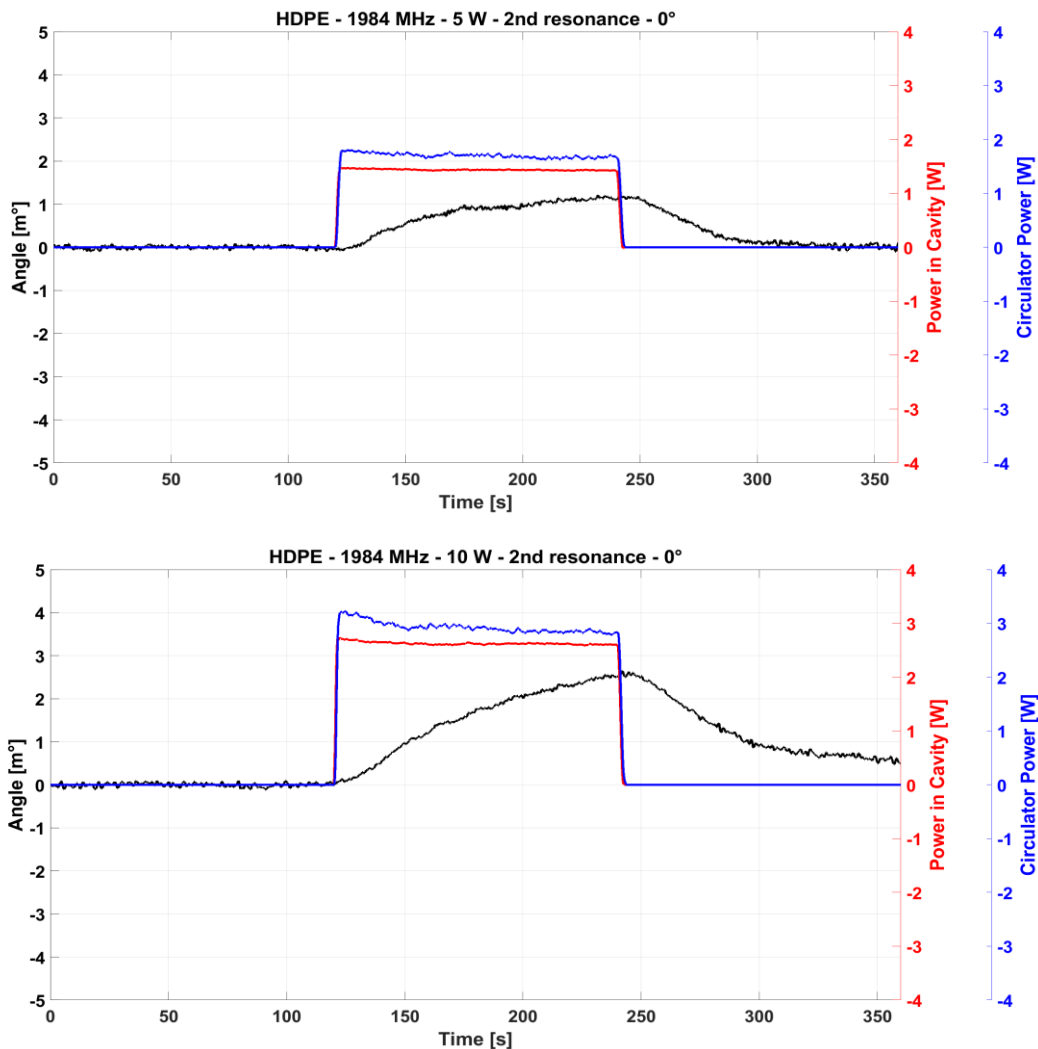


Figure 12. Function test of the rotational thrust balance.

Top: Measured signal of the angular encoder while operating the EMDrive at a frequency of 1984 MHz with 2 W of power inside the cavity (to be confirmed).

Bottom: Measured signal of the angular encoder while operating the EMDrive at a frequency of 1984 MHz with 2 W of power inside the cavity (to be confirmed).

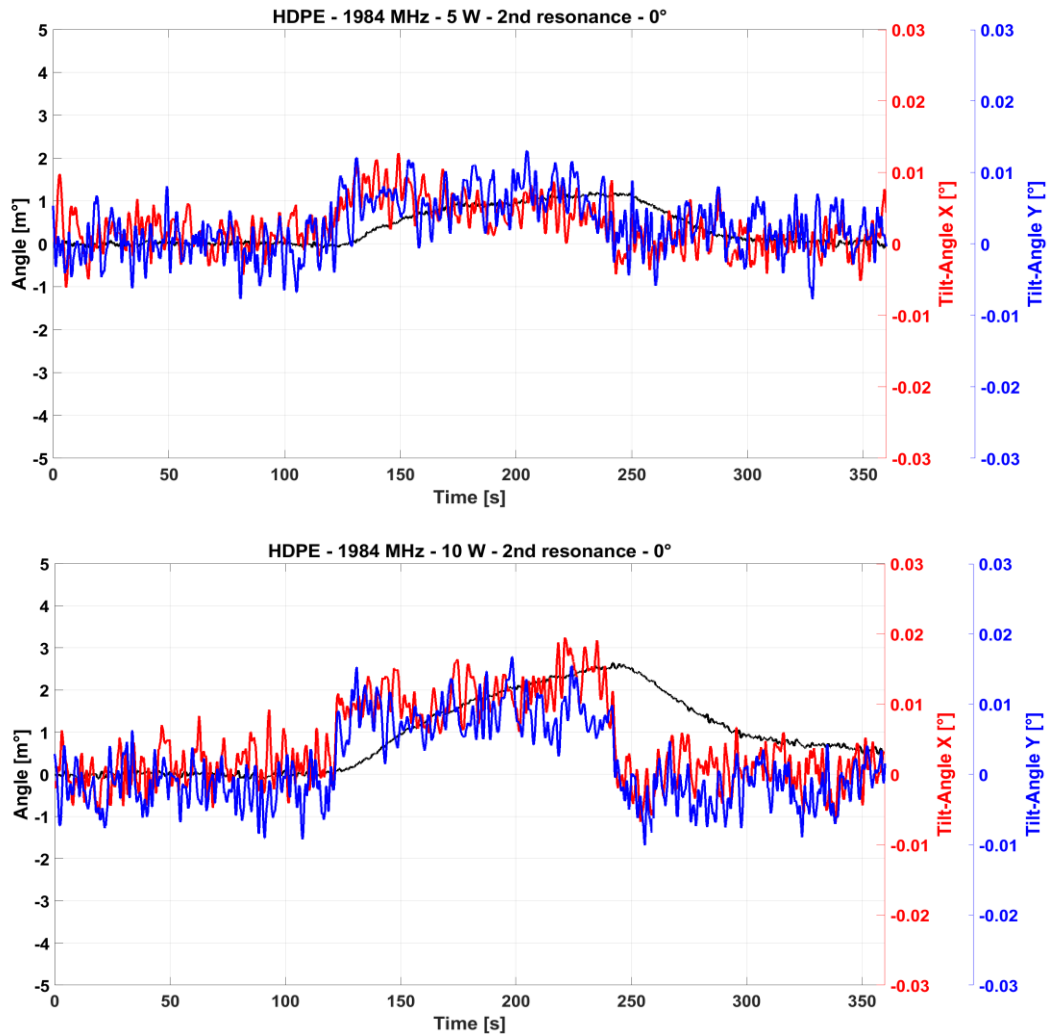


Figure 13. Function test of the rotating thrust balance.

Top: Measured signal of the angular encoder and tilt sensor while operating the EMDrive at a frequency of 1984 MHz with 2 W of power inside the cavity (to be confirmed).

Bottom: Measured signal of the angular encoder and tilt sensor while operating the EMDrive at a frequency of 1984 MHz with 2 W of power inside the cavity (to be confirmed).

In order to differentiate between rotation and deflection, the two available sensors operated simultaneously and observed the rotation as well as the tilt of the system. Due to these possibilities, the following results have to be treated with care, because they have to be verified with future tests.

The measurement process proceeded by switching the EMDrive into operational mode at two distinct position of the rotating structure. The first measurement was conducted at the starting position at an angular position defined as 0° (Fig. 12). With 5 W of power commanded to the EMDrive and a measured power within the cavity of 2 W at a frequency of 1984 MHz at the second resonance frequency, the angular sensor detected a motion of around 1 millidegree. A corresponding thrust cannot be calculated because the moment of inertia of the system was not calibrated for these preliminary function tests. Raising the commanded power to 10 W lead to a corresponding increase in the angular signal. It is important to mention, that these measurements have yet to be confirmed in future measurements. At this point, there is no assertion about the function of the EMDrive, but the verification of the thrust balances system components and communication in operation.

As described before, the signal could indicate a deflection rather than a circular motion. To verify this possibility, the signal delivered by the tilt sensor is layered above the encoder signal in figure 13. The sensor registered a tilt in one direction that increased with the commanded power as well, indicating the system deflected or shifted its center of mass. By moving the rotating system to the next position, defined as 180°, similar values of the deflection were obtained, but the signal orientation inverted. It is important to mention that every result presented was conducted at atmospheric pressure and outside of the vacuum chamber. According to the angular sensor resolution in the preliminary function tests, thrusts in the range of nN could be detected – at least for small deflections.

Every measurement presented in this chapter has yet to be confirmed in future measurements. The function test solely confirmed stable communication and data acquirement from the sensors of the rotational thrust balance, thus leading the way to combined measurements with the magnetic levitation.

V. Conclusion

The ability for a propulsion system to accelerate in a space-like environment leads to advantageous properties with respect to stationary thrust balances by visualizing the performance of mechanical work, thus removing possible doubts of the functionality of the concept.

The rotational thrust balance presented in this paper highlights the possibilities of the simple measurement principle, yet complex system requirements and testbed construction, which it brings along. Especially the continuous power supply during rotations with single-pins and a coaxial-connector offer a wide variety of propulsion concepts to be tested due to the adaptable supply interface and the independence of stored power on the testbed.

A detailed description of the most crucial components of the thrust balance was presented. After finishing the thermal tests for the cryostat, combined measurements of the whole system will be conducted and presented in future publications. Nevertheless, the superconductor is able to support loads of up to 22 kg with a margin of 8 kg for the thruster, that has been verified experimentally, which is magnitudes above other electromagnetically levitated testbeds.

The facility features a high precision optical encoder to track the angular position while performing full rotations with a resolution of up to 0.5 millidegree. The high resolution is able to detect nN of thrust if the bearing provides low enough friction. In order to provide full rotations for μN of thrust, a system for levelling of the rotational plane was presented.

Initial function tests of the thrust balance by operating it with the EMDrive were successful and confirmed the functionality of the communication system as well as data acquisition from the sensors. The results of these function tests were presented and have yet to be confirmed in future measurements. Nevertheless, the tests confirmed a high sensitivity of the sensors, leading the way for detailed characterizations of electric propulsion concepts.

Acknowledgments

We gratefully acknowledge the support for the SpaceDrive project by the German national space Agency DLR (Deutsches Zentrum fuer Luft- und Raumfahrttechnik) by funding from the Federal Ministry of Economic Affairs and Energy (BMWi) by approval from German Parliament (50RS1704).

References

- ¹M. Tajmar: *Advanced Space Propulsion Systems*, Springer Vienna, 2003
- ²Tajmar, M., and Fiedler, G., “Direct Thrust Measurements of an EMDrive and Evaluation of Possible Side Effects,” *51st AIAA/SAE/ASEE Joint Propulsion Conference*, 2015, p. AIAA 2015-4083. doi:10.2514/6.2015-4083
- ³Shawyer, R., “Second Generation EmDrive Propulsion Applied to SSTO Launcher and Interstellar Probe,” *Acta Astronautica*, vol. 116, 2015, pp. 166–174. doi:10.1016/j.actaastro.2015.07.002
- ⁴Woodward, J. F., “A New Experimental Approach to Mach’s Principle and Relativistic Graviation,” *Foundations of Physics Letters*, vol. 3, Oct. 1990, pp. 497–506. doi:10.1007/BF00665932
- ⁵Fearn, H., Zachar, A., Wanser, K., and Woodward, J., “Theory of a Mach Effect Thruster I,” *Journal of Modern Physics*, vol. 6, 2015, pp. 1510–1525. doi:10.4236/jmp.2015.611155
- ⁶M. Tajmar, M. Kößling, M. Weikert, M. Monette, *The SpaceDrive Project - Developing Revolutionary Propulsion at TU Dresden*, International Astronautical Congress, 2017.
- ⁷M. Tajmar, M. Kößling, M. Weikert, M. Monette, *The SpacDrive Project – First Results on EMDrive and Mach-Effect Thruster*, Space Propulsion, Seville, Spain, 14-18 May 2018, SP2018_016

⁸F. Mier-Hicks, P. C. Lozano, *Thrust Measurements of Ion Electrospray Thrusters using a CubeSat Compatible Magnetically Levitated Thrust Balance*, 34th International Electric Propulsion Conference, Hyogo-Kobe, Japan, 4 July 2015, IEPC-2015-148, ISTS-2015-b-148

⁹W. Buckel, R. Kleiner: *Superconductivity – Fundamentals and Applications*. Wiley-VCH, Second, Revised and Enlarged Edition, Weinheim, 2004